

# SPAD: Seven-Source Token Probability Attribution with Syntactic Aggregation for Detecting Hallucinations in RAG

Pengqian Lu, Jie Lu\*, Anjin Liu, and Guangquan Zhang

Australian Artificial Intelligence Institute (AAIL)

University of Technology Sydney

Ultimo, NSW 2007, Australia

{Pengqian.Lu@student., Jie.Lu@, Anjin.Liu@, Guangquan.Zhang@}uts.edu.au

## Abstract

Detecting hallucinations in Retrieval-Augmented Generation (RAG) remains a challenge. Prior approaches attribute hallucinations to a binary conflict between internal knowledge (stored in FFNs) and retrieved context. However, this perspective is incomplete, failing to account for the impact of other components in the generative process, such as the user query, previously generated tokens, the current token itself, and the final LayerNorm adjustment. To address this, we introduce SPAD. First, we mathematically attribute each token’s probability into seven distinct sources: Query, RAG, Past, Current Token, FFN, Final LayerNorm, and Initial Embedding. This attribution quantifies how each source contributes to the generation of the current token. Then, we aggregate these scores by POS tags to quantify how different components drive specific linguistic categories. By identifying anomalies, such as Nouns relying on Final LayerNorm, SPAD effectively detects hallucinations. Extensive experiments demonstrate that SPAD achieves state-of-the-art performance.

## 1 Introduction

Large Language Models (LLMs), despite their impressive capabilities, are prone to hallucinations (Huang et al., 2025). Consequently, Retrieval-Augmented Generation (RAG) (Lewis et al., 2020) is widely used to alleviate hallucinations by grounding models in external knowledge. However, RAG systems are not a panacea. They can still hallucinate by ignoring or misinterpreting the retrieved information (Sun et al., 2025). Detecting such failures is therefore a critical challenge.

The prevailing paradigm for hallucination detection often relies on hand-crafted proxy signals.

For example, common approaches measure output uncertainty via consistency checks (Manakul et al., 2023) or calculate the relative Mahalanobis distance of embeddings against a background corpus (Ren et al.). While efficient, these methods measure the symptoms of hallucination rather than its underlying architectural causes. Consequently, they often fail when a model is confidently incorrect (Kadavath et al., 2022).

To address the root cause of hallucination, recent research has shifted focus to the model’s internal representations. Pioneering works such as ReDeEP (Sun et al., 2025) assumes the RAG context is correct. They reveal that hallucinations in RAG typically stem from a dominance of internal parametric knowledge (stored in FFNs) over the retrieved external context.

This insight inspires a fundamental question: **Is the conflict between FFNs and RAG the only cause of hallucination?** Critical components like LayerNorm and the User Query are often overlooked. **Do contributions from these sources also drive hallucinations?** By decomposing the output into seven distinct information source, we obtain a complete attribution map. This enables detection based on comprehensive internal mechanics rather than partial proxy signals.

To achieve this, we also assume the RAG context contains relevant information and introduce SPAD (Seven-Source Token Probability Attribution with Syntactic Aggregation for Detecting Hallucinations in RAG). This framework mathematically attributes the final probability of each token to seven distinct sources: Query, RAG, Past, Current Token, FFN, Final LayerNorm, and Initial Embedding. The total attribution across these seven parts sums exactly to the token’s final probability, ensuring we capture the complete generation process.

However, raw attribution scores alone are insufficient for detection. A high reliance on internal knowledge (FFNs) does not necessarily imply a

\*Corresponding author.

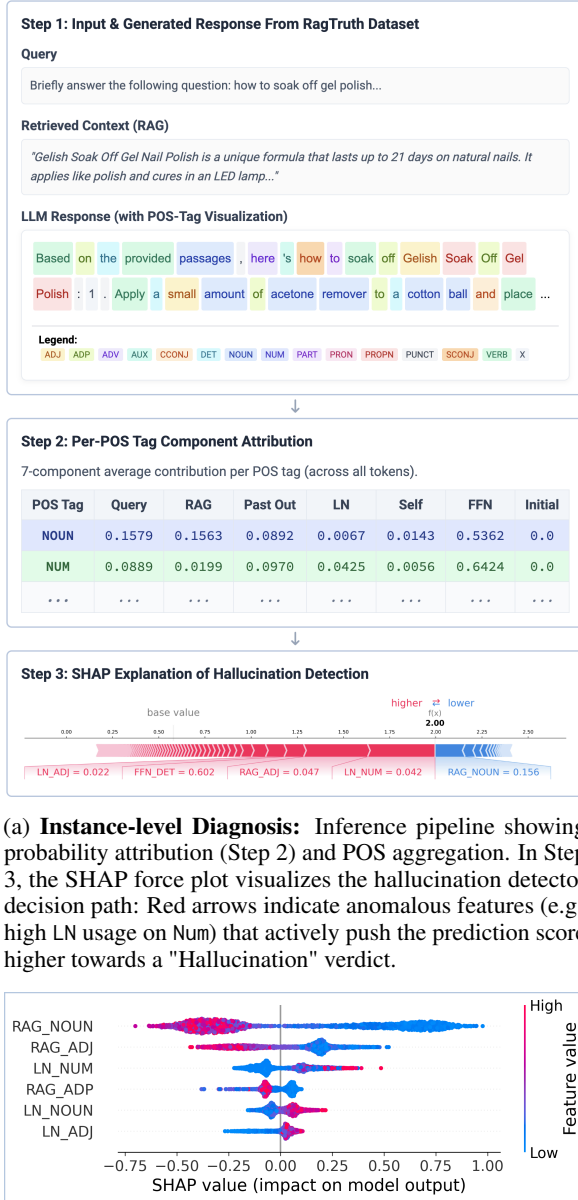


Figure 1: Applying SPAD framework to a Llama2-7b response from RagTruth dataset (Niu et al., 2024).

hallucination. This pattern is expected for function words like "the" or "of". Yet, it becomes highly suspicious when found in named entities. Therefore, treating all tokens equally fails to capture these critical distinctions.

To capture this distinction, we aggregate the attribution scores using Part-of-Speech (POS) tags. We select POS tags for their universality and ef-

ficiency, providing a robust feature space without the complexity of full dependency parsing.

Figure 1 illustrates SPAD detecting hallucinations on a Llama2-7b response (Touvron et al., 2023). As shown in Figure 1a, the pipeline attribute token probabilities to seven sources. These scores are then aggregated by POS tags and input into the classifier. The visualization in Step 3 highlights that the detection verdict is driven by specific syntax-source anomalies rather than generic signals. Figure 1b further validates this design by analyzing the feature importance of the trained classifier. The SHAP summary plot reveals that the most discriminative features are specific combinations of source and syntax. For instance, high RAG attribution on NOUNS correlates with factualness, while high LayerNorm attribution on NUM signals hallucination. This validates the necessity of syntax-aware source attribution. Our main contributions are:

1. We propose SPAD, a novel framework that mathematically attributes each token’s probability to seven distinct information sources. This provides a comprehensive mechanistic view of the token generation process.
2. We introduce a syntax-aware aggregation mechanism. By quantifying how information sources drive distinct parts of speech, this approach enables the detector to pinpoint anomalies in specific entities while ignoring benign grammatical patterns.
3. Extensive experiments demonstrate that SPAD achieves state-of-the-art performance. Our framework also offers transparent interpretability, automatically uncovering novel mechanistic signatures, such as anomalous LayerNorm contributions, that extend beyond the traditional FFN-RAG binary conflict.

## 2 Related Work

**Uncertainty and Proxy Metrics.** A prevalent approach involves detecting hallucinations via output uncertainty or proxy signals. Several methods quantify the inconsistency across multiple sampled responses or model ensembles to estimate uncertainty (Manakul et al., 2023; Malinin and Gales, 2021). To avoid the cost of multiple generations, others derive efficient proxy metrics from a single forward pass. These include utilizing energy scores or embedding distances (Liu et al., 2020;

Ren et al.), as well as measuring neighborhood instability or keyword-specific uncertainty (Lee et al., 2024; Zhang et al., 2023). While efficient, these methods primarily measure correlates of hallucination rather than analyzing the underlying generative mechanism.

**LLM-based Evaluation.** Another paradigm employs LLMs as external evaluators. In Retrieval-Augmented Generation (RAG), frameworks verify outputs against retrieved documents using claim extraction (Niu et al., 2024; Friel and Sanyal, 2023; Hu et al., 2024). Similarly, automated evaluation suites have been developed to systematically test for factual accuracy (Es et al., 2024; True-Lens, 2024; Ravichander et al., 2025). Alternatively, methods like cross-examination assess self-consistency without external knowledge (Cohen et al., 2023; Yehuda et al., 2024). Beyond prompting off-the-shelf models, (Su et al., 2025) proposed RL4HS to fine-tune LLMs via reinforcement learning for span-level hallucination detection. However, these approaches incur high computational costs due to external API calls or iterative generation steps, whereas our method is self-contained within the generating model.

**Probing Internal Activations.** Recent research investigates the model’s internal latent space for factuality signals. Seminal works identify linear “truthful directions” in activation space (Burns et al., 2022; Li et al., 2023), while others train probes to detect falsehoods even when outputs appear confident (Azaria and Mitchell, 2023; Han et al., 2024; Chen et al., 2024). Beyond passive detection, some approaches attribute behavior to specific components (Sun et al., 2025) or actively intervene in the decoding process. These interventions range from modifying activations during inference (Li et al., 2023) to re-ranking candidates based on internal state signatures (Chen et al., 2025; Zhang et al., 2025). Unlike these methods which often treat activations as aggregate features or modify generation, our work explicitly decomposes the final output probability. We trace the probability mass back to seven information sources providing a fine-grained and interpretable basis for detection.

### 3 Methodology

As illustrated in Figure 2, SPAD operates in three stages. We first derive an exact decomposition of token probabilities (Sec. 3.2), then attribute atten-

tion contributions to specific information sources (Sec. 3.3). Finally, we aggregate these scores to quantify how sources drive distinct parts of speech (Sec. 3.4). The pseudo-code and complexity analysis are provided in the Appendix. To provide the theoretical basis for our method, we first formalize the transformer’s residual architecture.

#### 3.1 Preliminaries: Residual Architecture

We analyze a standard decoder-only Transformer architecture, consisting of a stack of  $L$  layers. Given an input sequence  $\mathbf{x} = (x_1, \dots, x_T)$ , the model predicts the next token  $x_{T+1}$ .

##### 3.1.1 Residual Updates and Probing

The input tokens are mapped to continuous vectors via an embedding matrix  $\mathbf{W}_e \in \mathbb{R}^{V \times d}$  and summed with positional embeddings  $\mathbf{P}$ . The initial state is  $\mathbf{H}^{(0)} = \mathbf{W}_e[\mathbf{x}] + \mathbf{P}$ . We adopt the Pre-normalization (Pre-LN) configuration. Crucially, each layer  $l$  updates the hidden state via additive residual connections:

$$\mathbf{H}_{\text{mid}}^{(l)} = \mathbf{H}^{(l-1)} + \text{Attn}(\text{LN}(\mathbf{H}^{(l-1)})) \quad (1)$$

$$\mathbf{H}^{(l)} = \mathbf{H}_{\text{mid}}^{(l)} + \text{FFN}(\text{LN}(\mathbf{H}_{\text{mid}}^{(l)})) \quad (2)$$

This structure implies that the final representation is the sum of the initial embedding and all subsequent layer updates. To quantify these updates, we define a *Probe Function*  $\Phi(\mathbf{H}, y)$  similar with logit lens technique (nostalgebraist, 2020) that measures the hypothetical probability of the target token  $y$  given any intermediate state  $\mathbf{H}$ :

$$\Phi(\mathbf{H}, y) = \left[ \text{Softmax}(\mathbf{H}\mathbf{W}_e^\top) \right]_y \quad (3)$$

**Guiding Question:** *Since the model is a stack of residual updates, can we mathematically decompose the final probability exactly into the sum of component contributions?*

#### 3.2 Coarse-Grained Decomposition

We answer the preceding question affirmatively by leveraging the additive nature of the residual updates. Based on the probe function  $\Phi(\mathbf{H}, y)$  defined in Eq. (3), we isolate the probability contribution of each model component as the distinct change it induces in the probe output.

We define the baseline contribution from input static embeddings ( $\Delta P_{\text{initial}}$ ), the incremental gains from Attention and FFN blocks in layer  $l$

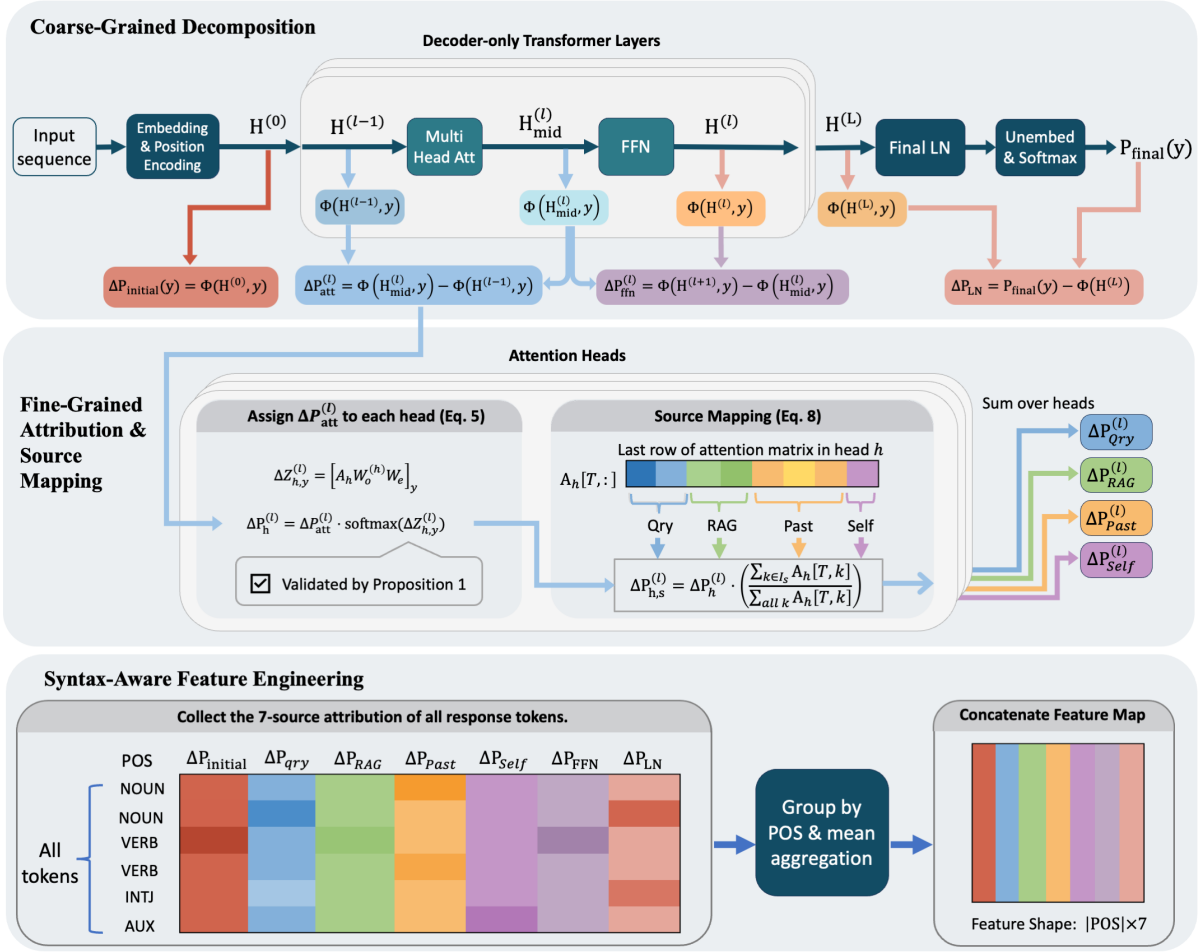


Figure 2: Overview of the SPAD framework. The attribution process consists of three progressive stages: (1) **Coarse-Grained Decomposition**: The final token probability is exactly decomposed into additive contributions from residual streams and LayerNorm components (Section 3.2). (2) **Fine-Grained Attribution & Source Mapping**: Attention contributions are apportioned to individual heads and subsequently mapped to four distinct input sources (Query, RAG, Past, Self) based on attention weights (Section 3.3). (3) **Syntax-Aware Feature Engineering**: These source-specific attributions are aggregated by POS tags to construct the final syntax-aware feature representation for hallucination detection (Section 3.3.4).

$(\Delta P_{\text{att}}^{(l)}, \Delta P_{\text{ffn}}^{(l)})$ , and the adjustment from the final LayerNorm ( $\Delta P_{\text{LN}}$ ) as follows:

$$\Delta P_{\text{initial}}(y) = \Phi(\mathbf{H}^{(0)}, y) \quad (4)$$

$$\Delta P_{\text{att}}^{(l)} = \Phi(\mathbf{H}_{\text{mid}}^{(l)}, y) - \Phi(\mathbf{H}^{(l-1)}, y) \quad (5)$$

$$\Delta P_{\text{ffn}}^{(l)} = \Phi(\mathbf{H}^{(l)}, y) - \Phi(\mathbf{H}_{\text{mid}}^{(l)}, y) \quad (6)$$

$$\Delta P_{\text{LN}} = P_{\text{final}}(y) - \Phi(\mathbf{H}^{(L)}, y) \quad (7)$$

By summing these telescoping differences, we derive the exact decomposition of the model’s output.

**Theorem 1** (Exact Probability Decomposition). *The final probability for a target token  $y$  is exactly the sum of the contribution from the initial embedding, the cumulative contributions from Attention and FFN blocks across all  $L$  layers, and the adjust-*

*ment from the final LayerNorm:*

$$P_{\text{final}}(y) = \Delta P_{\text{initial}}(y) + \Delta P_{\text{LN}} + \sum_{l=1}^L (\Delta P_{\text{att}}^{(l)} + \Delta P_{\text{ffn}}^{(l)}) \quad (8)$$

*Proof.* See Appendix.  $\square$

**The Guiding Question:** While Eq. (8) quantifies *how much* the model components contribute to the prediction probability, it treats the term  $\Delta P_{\text{att}}^{(l)}$  as a black box. To effectively detect hallucinations, we must identify *where* this attention is focused.

### 3.3 Fine-Grained Attribution

To identify the focus of attention, we must decompose the attention contribution  $\Delta P_{\text{att}}^{(l)}$  into contri-

butions from individual attention heads.

### 3.3.1 The Challenge: Non-Linearity

Standard Multi-Head Attention concatenates the outputs of  $H$  independent heads and projects them via an output matrix  $\mathbf{W}_O$ . Mathematically, by partitioning  $\mathbf{W}_O$  into head-specific sub-matrices, this operation is strictly equivalent to the sum of projected head outputs:

$$\mathbf{H}_{\text{att}}^{(l)} = \sum_{h=1}^H \underbrace{(\mathbf{A}_h \mathbf{V}_h)}_{\mathbf{h}_h} \mathbf{W}_O^{(h)} \quad (9)$$

where  $\mathbf{h}_h$  is the raw output of head  $h$ , derived from the layer input  $\mathbf{x}$ , the head-specific value projection  $\mathbf{V}_h$ , and the attention matrix  $\mathbf{A}_h$ .

Eq. (9) establishes that the attention output is linear with respect to individual heads in the hidden state space. However, our goal is to attribute the *probability* change  $\Delta P_{\text{att}}^{(l)}$  to each head. Since the probe function  $\Phi(\cdot)$  employs a non-linear Softmax operation, the sum of probability changes calculated by probing individual heads does not equal the attention block contribution:

$$\Delta P_{\text{att}}^{(l)} \neq \sum_{h=1}^H \left( \Phi(\mathbf{H}_{\text{input}} + \mathbf{h}_h \mathbf{W}_O^{(h)}) - \Phi(\mathbf{H}_{\text{input}}) \right) \quad (10)$$

This inequality prevents us from calculating head contributions by simply probing each head individually, motivating our shift to the logit space.

### 3.3.2 Logit-Based Apportionment

To bypass the non-linearity of the Softmax, we analyze contributions in the logit space, where additivity is preserved. Let  $\Delta z_{h,y}^{(l)}$  denote the scalar contribution of head  $h$  to the logit of the **target token**  $y$ . This is calculated as the dot product between the projected head output and the target token’s unembedding vector  $\mathbf{W}_{e,y}$ :

$$\Delta z_{h,y}^{(l)} = \left[ (\mathbf{A}_h \mathbf{V}_h) \mathbf{W}_O^{(h)} \right] \cdot \mathbf{W}_{e,y} \quad (11)$$

We then apportion the exact probability contribution  $\Delta P_{\text{att}}^{(l)}$  (derived in Section 3.2) to each head  $h$  proportional to its exponential logit contribution:

$$\Delta P_h^{(l)} = \Delta P_{\text{att}}^{(l)} \cdot \frac{\exp(\Delta z_{h,y}^{(l)})}{\sum_{j=1}^H \exp(\Delta z_{j,y}^{(l)})} \quad (12)$$

### 3.3.3 Theoretical Justification

Our strategy relies on the relationship between logit changes and probability updates. We rigorously establish this link via a first-order Taylor expansion.

**Proposition 1** (Gradient-Based Linear Decomposition). *The total probability contribution of the attention block,  $\Delta P_{\text{att}}^{(l)}$ , is approximated by the sum of head-specific logit contributions  $\Delta z_{h,y}^{(l)}$ , scaled by a layer-wide gradient factor:*

$$\Delta P_{\text{att}}^{(l)} \approx \mathcal{G}^{(l)} \cdot \sum_{h=1}^H \Delta z_{h,y}^{(l)} + \mathcal{E} \quad (13)$$

where  $\mathcal{G}^{(l)}$  is a common gradient term shared by all heads in layer  $l$ , and  $\mathcal{E}$  is the higher-order term.

*Proof.* See Appendix.  $\square$

While Proposition 1 suggests linearity, direct apportionment is numerically unstable. For instance, if positive and negative contributions across heads sum to near zero, the resulting weights would explode mathematically. Thus, Eq. (12) employs Softmax to avoid this problem.

#### Justification for First-Order Approximation.

We restrict our analysis to the first-order term for efficiency. Computing second-order Hessian interactions incurs a prohibitive  $\mathcal{O}(V^2)$  cost. Moreover, since LLMs are often “confidently incorrect” during hallucinations (Kadavath et al., 2022), the probability mass concentrates on the target, naturally suppressing the  $\mathcal{E}$ . Thus, the first-order approximation is both computationally necessary ( $\mathcal{O}(V)$ ) and sufficiently accurate.

### 3.3.4 Source Mapping and The 7-Source Split

Having isolated the head contribution  $\Delta P_h^{(l)}$ , we can now answer the guiding question by tracing attention back to input tokens using the attention matrix  $\mathbf{A}_h$ . We categorize inputs into four source types:  $\mathcal{S} = \{\text{Qry}, \text{RAG}, \text{Past}, \text{Self}\}$ . For a source type  $S$  containing token indices  $\mathcal{I}_S$ , the aggregated contribution is:

$$\Delta P_S^{(l)} = \sum_{h=1}^H \left( \Delta P_h^{(l)} \cdot \frac{\sum_{k \in \mathcal{I}_S} \mathbf{A}_h[T, k]}{\sum_{\text{all } k} \mathbf{A}_h[T, k]} \right) \quad (14)$$

By aggregating these components, we achieve a complete partition of the final probability  $P_{\text{final}}(y)$  into exactly seven distinct sources:

$$P_{\text{final}}(y) = P_{\text{initial}}(y) + \Delta P_{\text{LN}} + \sum_{l=1}^L \left( \Delta P_{\text{ffn}}^{(l)} + \sum_{S \in \mathcal{S}} \Delta P_S^{(l)} \right) \quad (15)$$

**The Guiding Question:** We have now derived a precise 7-dimensional attribution vector for every token. However, raw attribution scores lack context: a high  $P_{\text{FFN}}$  contribution might be normal for a function word but suspicious for a proper noun. How can we contextualize these scores with syntactic priors?

### 3.4 Syntax-Aware Feature Engineering

To resolve this ambiguity, we employ Part-of-Speech (POS) tagging as a lightweight syntactic prior. Specifically, we assign a POS tag by Spacy (Honnibal et al., 2020) to each generated token and aggregate the attribution scores for each grammatical category. By profiling which information sources (e.g., RAG) the LLM relies on for different parts of speech, we detect hallucination effectively.

#### 3.4.1 Tag Propagation Strategy

A mismatch problem arises because LLMs may split a word into multiple tokens while standard POS taggers process whole words. We resolve this via tag propagation: generated sub-word tokens inherit the POS tag of their parent word. For instance, if the noun “modification” is tokenized into [“modi”, “fication”], both sub-tokens are assigned the NOUN tag.

#### 3.4.2 Aggregation

We first define the attribution vector  $\mathbf{v}_t \in \mathbb{R}^7$  for each token  $x_t$  as the concatenation of its 7 source components derived in Section 3.3.4. To capture role-specific provenance patterns, we compute the mean attribution vector for each POS tag  $\tau$ :

$$\bar{\mathbf{v}}_\tau = \frac{1}{|\{t \mid \text{POS}(x_t) = \tau\}|} \sum_{t: \text{POS}(x_t) = \tau} \mathbf{v}_t \quad (16)$$

The final feature vector  $\mathbf{f} \in \mathbb{R}^{7 \times |\text{POS}|}$  is the concatenation of these POS-specific vectors. This representation combines *provenance* (source attribution) with *syntax* (linguistic structure), forming a robust basis for hallucination detection.

## 4 Experiments

### 4.1 Experimental Setup

We treat hallucination detection as a supervised binary classification task. We employ XGBoost (Chen and Guestrin, 2016) as our classifier, chosen for its efficiency and interpretability on tabular data. The input to the classifier is a 126-dimensional

syntax-aware feature vector, constructed by aggregating the 7-source attribution scores across 18 universal POS tags (e.g., NOUN, VERB) defined by SpaCy (Honnibal et al., 2020). To ensure rigorous evaluation and reproducibility, we implement strict data isolation protocols (e.g., stratified cross-validation) tailored to the data availability of each task. See implementation details in Appendix.

### 4.2 Dataset and Baselines

To ensure a fair comparison, we utilize the public RAG hallucination benchmark established by (Sun et al., 2025). This benchmark comprises human-annotated responses from Llama2 (7B/13B) and Llama3 (8B) across two datasets: **RAGTruth** (QA, Data-to-Text, Summarization) and **Dolly** (Summarization, Closed-QA). Implementation details are provided in Appendix. We compare our method against representative approaches from three categories introduced in Section 2. The introduction of baseliens are provided in Appendix.

### 4.3 Comparison with Baselines

The main experimental results, presented in Table 1, demonstrate that our proposed attribution-based framework achieves superior performance across the majority of experimental settings, significantly outperforming baselines on the large-scale benchmark while maintaining strong competitiveness on low-resource datasets.

On the comprehensive RAGTruth benchmark, our method demonstrates a clear advantage. For instance, with the Llama2-7B model, our detector achieves an F1-score of 0.7218 and an AUC of 0.7839, surpassing the strongest competitor, ReDeEP, which scored 0.7190 and 0.7458, respectively. This trend is amplified with the larger Llama2-13B model, where we attain the highest F1-score (0.7912) and AUC (0.8685). The performance gap is evident on the newer Llama3-8B model, where our framework leads by a substantial margin, achieving an F1-score of 0.7975 compared to the next-best 0.6986 from LMVLM. These results on a sufficiently large dataset robustly validate our core hypothesis: a complete, syntax-aware attribution map provides a richer feature space for identifying hallucinations than methods relying on limited proxy signals.

The Dolly (AC) dataset presents a more challenging scenario due to its extreme data scarcity (only 100 test samples). Despite this, our method demonstrates remarkable adaptability. On the

Method	RAGTruth								
	LLaMA2-7B			LLaMA2-13B			LLaMA3-8B		
	AUC	Recall	F1	AUC	Recall	F1	AUC	Recall	F1
SelfCheckGPT (Manakul et al., 2023)	—	0.4642	0.4642	—	0.4642	0.4642	—	0.5111	0.5111
Perplexity (Ren et al.)	0.5091	0.5190	0.6749	0.5091	0.5190	0.6749	0.6235	0.6537	0.6778
LN-Entropy (Malinin and Gales, 2021)	0.5912	0.5383	0.6655	0.5912	0.5383	0.6655	0.7021	0.5596	0.6282
Energy (Liu et al., 2020)	0.5619	0.5057	0.6657	0.5619	0.5057	0.6657	0.5959	0.5514	0.6720
Focus (Zhang et al., 2023)	0.6233	0.5309	0.6622	0.7888	0.6173	0.6977	0.6378	0.6688	0.6879
Prompt (Niu et al., 2024)	—	0.7200	0.6720	—	0.7000	0.6899	—	0.4403	0.5691
LMVLM (Cohen et al., 2023)	—	0.7389	0.6473	—	<b>0.8357</b>	0.6553	—	0.5109	<u>0.6986</u>
ChainPoll (Friel and Sanyal, 2023)	0.6738	0.7832	0.7066	0.7414	<u>0.7874</u>	0.7342	0.6687	0.4486	0.5813
RAGAS (Es et al., 2024)	0.7290	0.6327	0.6667	0.7541	0.6763	0.6747	0.6776	0.3909	0.5094
Trulens (TrueLens, 2024)	0.6510	0.6814	0.6567	0.7073	0.7729	0.6867	0.6464	0.3909	0.5053
RefCheck (Hu et al., 2024)	0.6912	0.6280	0.6736	0.7857	0.6800	0.7023	0.6014	0.3580	0.4628
P(True) (Kadavath et al., 2022)	0.7093	0.5194	0.5313	0.7998	0.5980	0.7032	0.6323	0.7083	0.6835
EigenScore (Chen et al., 2024)	0.6045	0.7469	0.6682	0.6640	0.6715	0.6637	0.6497	0.7078	0.6745
SEP (Han et al., 2024)	0.7143	0.7477	0.6627	0.8089	0.6580	0.7159	0.7004	0.7333	0.6915
SAPLMA (Azaria and Mitchell, 2023)	0.7037	0.5091	0.6726	0.8029	0.5053	0.6529	0.7092	0.5432	0.6718
ITI (Li et al., 2023)	0.7161	0.5416	0.6745	0.8051	0.5519	0.6838	0.6534	0.6850	0.6933
ReDeEP (Sun et al., 2025)	<u>0.7458</u>	<u>0.8097</u>	0.7190	<u>0.8244</u>	0.7198	<u>0.7587</u>	<u>0.7285</u>	<u>0.7819</u>	0.6947
<b>SPAD</b>	<b>0.7839</b>	<b>0.8496</b>	<b>0.7218</b>	<b>0.8685</b>	0.7778	<b>0.7912</b>	<b>0.8148</b>	<b>0.7975</b>	<b>0.7975</b>

Method	Dolly (AC)								
	LLaMA2-7B			LLaMA2-13B			LLaMA3-8B		
	AUC	Recall	F1	AUC	Recall	F1	AUC	Recall	F1
SelfCheckGPT (Manakul et al., 2023)	—	0.1897	0.3188	0.2728	0.1897	0.3188	0.1095	0.2195	0.3600
Perplexity (Ren et al.)	0.2728	0.7719	0.7097	0.2728	0.7719	0.7097	0.1095	0.3902	0.4571
LN-Entropy (Malinin and Gales, 2021)	0.2904	0.7368	0.6772	0.2904	0.7368	0.6772	0.1150	0.5365	0.5301
Energy (Liu et al., 2020)	0.2179	0.6316	0.6261	0.2179	0.6316	0.6261	-0.0678	0.4047	0.4440
Focus (Zhang et al., 2023)	0.3174	0.5593	0.6534	0.1643	0.7333	0.6168	0.1266	0.6918	0.6874
Prompt (Niu et al., 2024)	—	0.3965	0.5476	—	0.4182	0.5823	—	0.3902	0.5000
LMVLM (Cohen et al., 2023)	—	0.7759	0.7200	—	0.7273	0.6838	—	0.6341	0.5361
ChainPoll (Friel and Sanyal, 2023)	0.3502	0.4138	0.5581	0.4758	0.4364	0.6000	0.2691	0.3415	0.4516
RAGAS (Es et al., 2024)	0.2877	0.5345	0.6392	0.2840	0.4182	0.5476	0.3628	<u>0.8000</u>	0.5246
Trulens (TrueLens, 2024)	0.3198	0.5517	0.6667	0.2565	0.3818	0.4941	0.3352	0.3659	0.5172
RefCheck (Hu et al., 2024)	0.2494	0.3966	0.5412	0.2869	0.2545	0.3944	-0.0089	0.1951	0.2759
P(True) (Kadavath et al., 2022)	0.1987	0.6350	0.6509	0.2009	0.6180	0.5739	0.3472	0.5707	0.6573
EigenScore (Chen et al., 2024)	0.2428	0.7500	0.7241	0.2948	0.8181	0.7200	0.2065	0.7142	0.5952
SEP (Han et al., 2024)	0.2605	0.6216	0.7023	0.2823	0.6545	0.6923	0.0639	0.6829	0.6829
SAPLMA (Azaria and Mitchell, 2023)	0.0179	0.5714	0.7179	0.2006	0.6000	0.6923	-0.0327	0.4040	0.5714
ITI (Li et al., 2023)	0.0442	0.5816	0.6281	0.0646	0.5385	0.6712	0.0024	0.3091	0.4250
ReDeEP (Sun et al., 2025)	<u>0.5136</u>	<b>0.8245</b>	<b>0.7833</b>	<u>0.5842</u>	<u>0.8518</u>	<u>0.7603</u>	<u>0.3652</u>	<b>0.8392</b>	<u>0.7100</u>
<b>SPAD</b>	<b>0.6514</b>	<u>0.7931</u>	<u>0.7541</u>	<b>0.7848</b>	<b>0.9444</b>	<b>0.7907</b>	<b>0.7717</b>	0.7073	<b>0.7733</b>

Table 1: Results on RAGTruth and Dolly (AC) datasets across three LLaMA models. We report AUC, Recall, and F1-score. Bold values indicate the best performance and underlined values indicate the second-best.

Llama2-13B model, our approach sweeps all three metrics with a commanding lead, achieving the highest AUC (0.7848), Recall (0.9444), and F1-score (0.7907), significantly outperforming previous state-of-the-art baselines. Similarly, on the Llama3-8B model, our method reinforces its superiority, securing the best-in-class F1-score (0.7733) and a dominant AUC (0.7717). For the Llama2-7B model, while simpler baselines like ReDeEP yield a slightly higher F1-score, our method retains the highest AUC (0.6514). This suggests that while determining the optimal classification threshold is inherently difficult with extremely limited training

samples, our framework consistently captures the most discriminative features for ranking truthful and hallucinated responses.

#### 4.4 Interpretability Analysis

Beyond performance metrics, we seek to understand the mechanistic logic driving detection. We apply SHAP analysis to the classifiers trained on the RAGTruth benchmark. The Dolly dataset is excluded due to its small size. Three observations are obtained from this analysis.

**1. The syntax of grounding varies by architecture.** While RAG attribution is universally critical

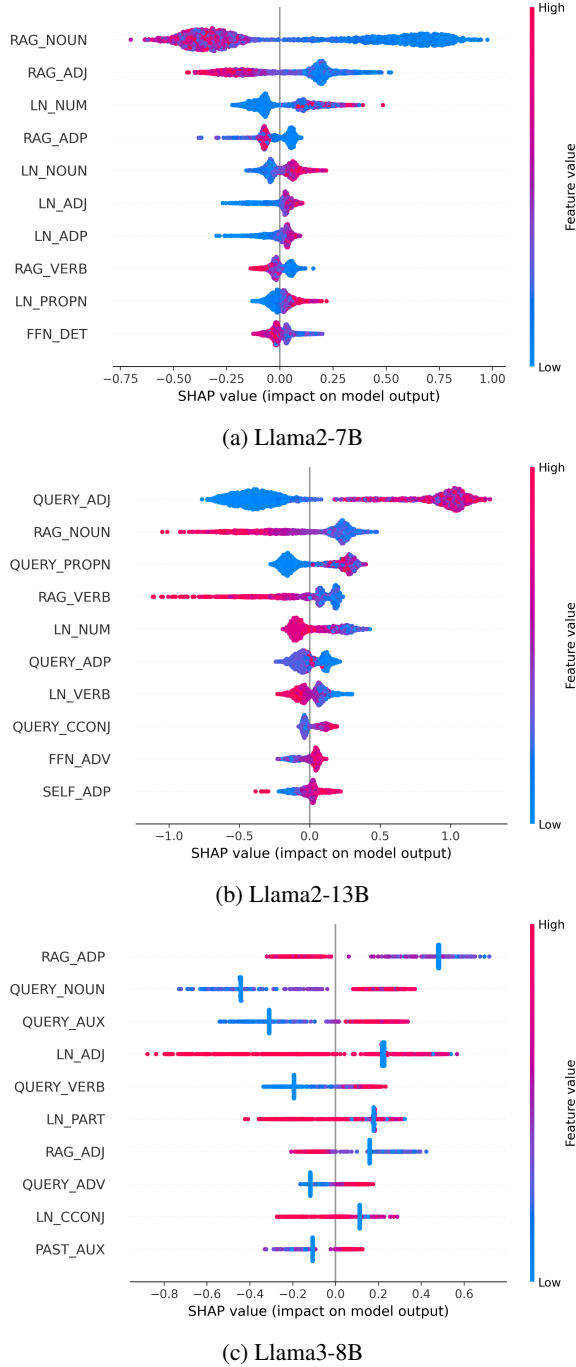


Figure 3: SHAP summary plots illustrating the decision logic. We visualize the top-10 features for classifiers trained on the RAGTruth subsets corresponding to Llama2-7B, Llama2-13B, and Llama3-8B. The x-axis represents the SHAP value, where positive values indicate a push towards classifying the response as a Hallucination. The color represents the feature value (Red = High attribution, Blue = Low).

for factuality, the specific POS tags carrying this signal change. Llama2 models (7B/13B) rely primarily on content words, with RAG\_NOUN being the top predictor. In contrast, Llama3-8B relies on re-

lational structures, with RAG\_ADP (Adpositions like "by") emerging as the most discriminative feature.

**2. LayerNorm on Numerals is a critical but flip-flopping signal.** The Final LayerNorm (LN) plays a major role in numerical reasoning, but its effect reverses across models. In Llama2-7B, high LN\_NUM attribution acts as a warning sign for hallucination. However, in Llama2-13B, high LN\_NUM indicates factuality. This difference shows that detection must capture model-specific behaviors.

**3. The User Query is an overlooked but critical hallucination driver.** Query-based features frequently rank among the top predictors, challenging the traditional focus on just RAG and FFNs. In Llama2-13B and Llama3-8B, features like QUERY\_ADJ and QUERY\_NOUN appear in the top-3 most important features. This result shows that monitoring the model’s reliance on the prompt is as vital as monitoring the retrieved context.

## 5 Limitations

Our framework presents three limitations. First, it relies on **white-box access** to model internals, preventing application to closed-source APIs. Second, the decomposition incurs higher **computational overhead** than simple scalar probes. However, it remains significantly more efficient than sampling-based or LLM-as-a-Judge methods as our method requires only a single forward pass. Third, our feature engineering depends on **external linguistic tools** (POS taggers), which may limit generalization to specialized domains like code generation where standard syntax is less defined.

## 6 Conclusion and Future Work

We introduced SPAD to attribute token probability into seven distinct sources. By combining these with syntax-aware features, our framework effectively detects RAG hallucinations and outperforms baselines. Our results show that hallucination signals vary across models. This confirms the need for a learnable approach rather than static heuristics.

Our future work will focus on two directions. First, we plan to extend our attribution framework to semantic phrases to achieve more efficient and effective detection. Second, we aim to implement active hallucination mitigation by monitoring contributions in real time to suppress risky sources and correct the generation process.

## Acknowledgements

This work was supported by the Australian Research Council through the Laureate Fellow Project under Grant FL190100149.

## References

- Takuya Akiba, Shotaro Sano, Toshihiko Yanase, Takeru Ohta, and Masanori Koyama. 2019. Optuna: A next-generation hyperparameter optimization framework. In *Proceedings of the 25th ACM SIGKDD International Conference on Knowledge Discovery and Data Mining*.
- Amos Azaria and Tom Mitchell. 2023. The internal state of an llm knows when it’s lying. In *Findings of the Association for Computational Linguistics: EMNLP 2023*, pages 967–976.
- Collin Burns, Haotian Ye, Dan Klein, and Jacob Steinhardt. 2022. Discovering latent knowledge in language models without supervision. *arXiv preprint arXiv:2212.03827*.
- Chao Chen, Kai Liu, Ze Chen, Yi Gu, Yue Wu, Mingyuan Tao, Zhihang Fu, and Jieping Ye. 2024. Inside: LLMs’ internal states retain the power of hallucination detection.
- Tianqi Chen and Carlos Guestrin. 2016. Xgboost: A scalable tree boosting system. In *Proceedings of the 22nd acm sigkdd international conference on knowledge discovery and data mining*, pages 785–794.
- Yuyan Chen, Zehao Li, Shuangjie You, Zhengyu Chen, Jingwen Chang, Yi Zhang, Weinan Dai, Qingpei Guo, and Yanghua Xiao. 2025. Attributive reasoning for hallucination diagnosis of large language models. In *Proceedings of the AAAI Conference on Artificial Intelligence*, volume 39, pages 23660–23668.
- Roi Cohen, May Hamri, Mor Geva, and Amir Globerson. 2023. Lm vs lm: Detecting factual errors via cross examination. In *Proceedings of the 2023 Conference on Empirical Methods in Natural Language Processing*, pages 12621–12640.
- Shahul Es, Jithin James, Luis Espinosa Anke, and Steven Schockaert. 2024. Ragas: Automated evaluation of retrieval augmented generation. In *Proceedings of the 18th Conference of the European Chapter of the Association for Computational Linguistics: System Demonstrations*, pages 150–158.
- Robert Friel and Atindriyo Sanyal. 2023. Chainpoll: A high efficacy method for llm hallucination detection. *arXiv preprint arXiv:2310.18344*.
- Aaron Grattafiori, Abhimanyu Dubey, Abhinav Jauhri, Abhinav Pandey, Abhishek Kadian, Ahmad Al-Dahle, Aiesha Letman, Akhil Mathur, Alan Schelten, Alex Vaughan, and 1 others. 2024. The llama 3 herd of models. *arXiv preprint arXiv:2407.21783*.
- Jiatong Han, Jannik Kossen, Muhammed Razzak, Lisa Schut, Shreshth A Malik, and Yarin Gal. 2024. Semantic entropy probes: Robust and cheap hallucination detection in llms. In *ICML 2024 Workshop on Foundation Models in the Wild*.
- Matthew Honnibal, Ines Montani, Sofie Van Landeghem, Adriane Boyd, and 1 others. 2020. spacy: Industrial-strength natural language processing in python.
- Xiangkun Hu, Dongyu Ru, Lin Qiu, Qipeng Guo, Tianhang Zhang, Yang Xu, Yun Luo, Pengfei Liu, Yue Zhang, and Zheng Zhang. 2024. Refchecker: Reference-based fine-grained hallucination checker and benchmark for large language models. *arXiv preprint arXiv:2405.14486*.
- Lei Huang, Weijiang Yu, Weitao Ma, Weihong Zhong, Zhangyin Feng, Haotian Wang, Qianglong Chen, Weihua Peng, Xiaocheng Feng, Bing Qin, and 1 others. 2025. A survey on hallucination in large language models: Principles, taxonomy, challenges, and open questions. *ACM Transactions on Information Systems*, 43(2):1–55.
- Saurav Kadavath, Tom Conerly, Amanda Askell, Tom Henighan, Dawn Drain, Ethan Perez, Nicholas Schiefer, Zac Hatfield-Dodds, Nova DasSarma, Eli Tran-Johnson, and 1 others. 2022. Language models (mostly) know what they know. *arXiv preprint arXiv:2207.05221*.
- Hakyung Lee, Keon-Hee Park, Hoyoon Byun, Jeyoon Yeom, Jihee Kim, Gyeong-Moon Park, and Kyungwoo Song. 2024. Ced: Comparing embedding differences for detecting out-of-distribution and hallucinated text. In *Findings of the Association for Computational Linguistics: EMNLP 2024*, pages 14866–14882.
- Patrick Lewis, Ethan Perez, Aleksandra Piktus, Fabio Petroni, Vladimir Karpukhin, Naman Goyal, Heinrich Küttler, Mike Lewis, Wen-tau Yih, Tim Rocktäschel, and 1 others. 2020. Retrieval-augmented generation for knowledge-intensive nlp tasks. *Advances in neural information processing systems*, 33:9459–9474.
- Kenneth Li, Oam Patel, Fernanda Viégas, Hanspeter Pfister, and Martin Wattenberg. 2023. Inference-time intervention: Eliciting truthful answers from a language model. *Advances in Neural Information Processing Systems*, 36:41451–41530.
- Weitang Liu, Xiaoyun Wang, John Owens, and Yixuan Li. 2020. Energy-based out-of-distribution detection. *Advances in neural information processing systems*, 33:21464–21475.
- Andrey Malinin and Mark Gales. 2021. Uncertainty estimation in autoregressive structured prediction. In *International Conference on Learning Representations*.

Potsawee Manakul, Adian Liusie, and Mark Gales. 2023. Selfcheckgpt: Zero-resource black-box hallucination detection for generative large language models. In *Proceedings of the 2023 conference on empirical methods in natural language processing*, pages 9004–9017.

Cheng Niu, Yuanhao Wu, Juno Zhu, Siliang Xu, Kashun Shum, Randy Zhong, Juntong Song, and Tong Zhang. 2024. Ragtruth: A hallucination corpus for developing trustworthy retrieval-augmented language models. In *Proceedings of the 62nd Annual Meeting of the Association for Computational Linguistics (Volume 1: Long Papers)*, pages 10862–10878.

nostalgebraist. 2020. [interpreting gpt: the logit lens](#). LessWrong.

F. Pedregosa, G. Varoquaux, A. Gramfort, V. Michel, B. Thirion, O. Grisel, M. Blondel, P. Prettenhofer, R. Weiss, V. Dubourg, J. Vanderplas, A. Passos, D. Cournapeau, M. Brucher, M. Perrot, and E. Duchesnay. 2011. Scikit-learn: Machine learning in Python. *Journal of Machine Learning Research*, 12:2825–2830.

Abhilasha Ravichander, Shruti Ghela, David Wadden, and Yejin Choi. 2025. Halogen: Fantastic llm hallucinations and where to find them. *arXiv preprint arXiv:2501.08292*.

Jie Ren, Jiaming Luo, Yao Zhao, Kundan Krishna, Mohammad Saleh, Balaji Lakshminarayanan, and Peter J Liu. Out-of-distribution detection and selective generation for conditional language models. In *The Eleventh International Conference on Learning Representations*.

Hsuan Su, Ting-Yao Hu, Hema Swetha Koppula, Kundan Krishna, Hadi Pouransari, Cheng-Yu Hsieh, Cem Koc, Joseph Yitan Cheng, Oncel Tuzel, and Raviteja Vemulapalli. 2025. Learning to reason for hallucination span detection. *arXiv preprint arXiv:2510.02173*.

Zhongxiang Sun, Xiaoxue Zang, Kai Zheng, Jun Xu, Xiao Zhang, Weijie Yu, Yang Song, and Han Li. 2025. Redeeep: Detecting hallucination in retrieval-augmented generation via mechanistic interpretability. In *ICLR*.

Hugo Touvron, Louis Martin, Kevin Stone, Peter Albert, Amjad Almahairi, Yasmine Babaei, Nikolay Bashlykov, Soumya Batra, Prajjwal Bhargava, Shruti Bhosale, and 1 others. 2023. Llama 2: Open foundation and fine-tuned chat models. *arXiv preprint arXiv:2307.09288*.

TrueLens. 2024. [Truelens: Evaluate and track llm applications](#).

Yakir Yehuda, Itzik Malkiel, Oren Barkan, Jonathan Weill, Royi Ronen, and Noam Koenigstein. 2024. Interrogatellm: Zero-resource hallucination detection in llm-generated answers. In *Proceedings of the 62nd Annual Meeting of the Association for Computational*

*Linguistics (Volume 1: Long Papers)*, pages 9333–9347.

Fujie Zhang, Peiqi Yu, Biao Yi, Baolei Zhang, Tong Li, and Zheli Liu. 2025. Prompt-guided internal states for hallucination detection of large language models. In *Proceedings of the 63rd Annual Meeting of the Association for Computational Linguistics (Volume 1: Long Papers)*, pages 21806–21818.

Tianhang Zhang, Lin Qiu, Qipeng Guo, Cheng Deng, Yue Zhang, Zheng Zhang, Chenghu Zhou, Xinbing Wang, and Luoyi Fu. 2023. Enhancing uncertainty-based hallucination detection with stronger focus. In *Proceedings of the 2023 Conference on Empirical Methods in Natural Language Processing*, pages 915–932.

## A Proof of Theorem 1

We expand the right-hand side (RHS) of Eq. 8 by substituting the definitions of each term.

First, consider the summation term. By substituting  $\Delta P_{\text{att}}^{(l)}$  and  $\Delta P_{\text{ffn}}^{(l)}$ , the intermediate probe value  $\Phi(\mathbf{H}_{\text{mid}}^{(l)})$  cancels out within each layer:

$$\begin{aligned} & \sum_{l=1}^L (\Delta P_{\text{att}}^{(l)} + \Delta P_{\text{ffn}}^{(l)}) \\ &= \sum_{l=1}^L ([\Phi(\mathbf{H}_{\text{mid}}^{(l)}) - \Phi(\mathbf{H}^{(l-1)})] + [\Phi(\mathbf{H}^{(l)}) - \Phi(\mathbf{H}_{\text{mid}}^{(l)})]) \\ &= \sum_{l=1}^L (\Phi(\mathbf{H}^{(l)}) - \Phi(\mathbf{H}^{(l-1)})) \end{aligned}$$

This summation forms a telescoping series where adjacent terms cancel:

$$\begin{aligned} & \sum_{l=1}^L (\Phi(\mathbf{H}^{(l)}) - \Phi(\mathbf{H}^{(l-1)})) \\ &= (\Phi(\mathbf{H}^{(1)}) - \Phi(\mathbf{H}^{(0)})) + \dots \\ &+ (\Phi(\mathbf{H}^{(L)}) - \Phi(\mathbf{H}^{(L-1)})) \\ &= \Phi(\mathbf{H}^{(L)}) - \Phi(\mathbf{H}^{(0)}) \end{aligned}$$

Now, substituting this result, along with the definitions of  $P_{\text{initial}}$  and  $\Delta P_{\text{LN}}$ , back into the full RHS expression:

$$\begin{aligned} \text{RHS} &= \underbrace{\Phi(\mathbf{H}^{(0)})}_{P_{\text{initial}}} + \underbrace{(P_{\text{final}} - \Phi(\mathbf{H}^{(L)}))}_{\Delta P_{\text{LN}}} \\ &+ \underbrace{(\Phi(\mathbf{H}^{(L)}) - \Phi(\mathbf{H}^{(0)}))}_{\text{Summation}} = P_{\text{final}} \end{aligned}$$

The RHS simplifies exactly to  $P_{\text{final}}(y)$ , which completes the proof.

## B Proof of Proposition 1

*Proof.* We consider the  $l$ -th layer of the Transformer. Let  $\mathbf{H}^{(l-1)} \in \mathbb{R}^d$  be the input hidden state. The Multi-Head Attention mechanism computes a residual update  $\Delta\mathbf{H}$  by summing the outputs of  $H$  heads:

$$\Delta\mathbf{H} = \sum_{h=1}^H \mathbf{h}_h \quad (17)$$

where  $\mathbf{h}_h \in \mathbb{R}^d$  is the projected output of the  $h$ -th head.

The probe function  $\Phi(\mathbf{H}, y)$  computes the probability of the target token  $y$  by projecting the hidden state onto the vocabulary logits  $\mathbf{z} \in \mathbb{R}^V$  and applying the Softmax function:

$$\Phi(\mathbf{H}, y) = \frac{\exp(\mathbf{z}_y)}{\sum_{v=1}^V \exp(\mathbf{z}_v)}, \quad \text{where } \mathbf{z}_v = \mathbf{H} \cdot \mathbf{w}_{e,v} \quad (18)$$

Here,  $\mathbf{w}_{e,v}$  is the unembedding vector for token  $v$  from matrix  $\mathbf{W}_e$ . For brevity, let  $p_y = \Phi(\mathbf{H}^{(l-1)}, y)$  denote the probability of the target token at the current state.

We approximate the change in probability,  $\Delta P_{\text{att}}^{(l)}$ , using a first-order Taylor expansion of  $\Phi$  with respect to  $\mathbf{H}$  around  $\mathbf{H}^{(l-1)}$ :

$$\begin{aligned} \Delta P_{\text{att}}^{(l)} &= \Phi(\mathbf{H}^{(l-1)} + \Delta\mathbf{H}, y) - \Phi(\mathbf{H}^{(l-1)}, y) \\ &\approx \nabla_{\mathbf{H}} \Phi(\mathbf{H}^{(l-1)}, y)^\top \cdot \Delta\mathbf{H} \\ &= \sum_{h=1}^H \left( \nabla_{\mathbf{H}} \Phi(\mathbf{H}^{(l-1)}, y)^\top \cdot \mathbf{h}_h \right) \end{aligned} \quad (19)$$

To compute the gradient  $\nabla_{\mathbf{H}} \Phi$ , we apply the chain rule through the logits  $z_v$ . The partial derivative of the Softmax output  $p_y$  with respect to any logit  $z_v$  is given by  $p_y(\delta_{yv} - p_v)$ , where  $\delta$  is the Kronecker delta. The gradient of the logit  $z_v$  with respect to  $\mathbf{H}$  is simply  $\mathbf{w}_{e,v}$ . Thus:

$$\begin{aligned} \nabla_{\mathbf{H}} \Phi &= \sum_{v=1}^V \frac{\partial \Phi}{\partial z_v} \frac{\partial z_v}{\partial \mathbf{H}} \\ &= \sum_{v=1}^V p_y(\delta_{yv} - p_v) \mathbf{w}_{e,v} \\ &= p_y(1 - p_y) \mathbf{w}_{e,y} - \sum_{v \neq y} p_y p_v \mathbf{w}_{e,v} \end{aligned} \quad (20)$$

Substituting this gradient back into Eq. (19) for a

specific head contribution term (denoted as  $\text{Term}_h$ ):

$$\begin{aligned} \text{Term}_h &= \nabla_{\mathbf{H}} \Phi^\top \cdot \mathbf{h}_h \\ &= \underbrace{p_y(1 - p_y)}_{\mathcal{G}^{(l)}} (\mathbf{w}_{e,y}^\top \cdot \mathbf{h}_h) - \underbrace{\sum_{v \neq y} p_y p_v (\mathbf{w}_{e,v}^\top \cdot \mathbf{h}_h)}_{\mathcal{E}_h} \end{aligned} \quad (21)$$

We observe that the dot product  $\mathbf{w}_{e,y}^\top \cdot \mathbf{h}_h$  is strictly equivalent to the scalar logit contribution  $\Delta z_{h,y}^{(l)}$  defined in Eq. (7). The factor  $\mathcal{G}^{(l)} = p_y(1 - p_y)$  represents the gradient common to all heads, depending only on the layer input  $\mathbf{H}^{(l-1)}$ . Therefore, the contribution of head  $h$  is dominated by the linear term  $\mathcal{G}^{(l)} \cdot \Delta z_{h,y}^{(l)}$ , subject to the off-target error term  $\mathcal{E}_h$ .  $\square$

## C Implementation Details

**Environment and Models.** All experiments were conducted on a computational node equipped with an NVIDIA A100 GPU and 200GB of RAM. We evaluate our framework using three Large Language Models: Llama2-7b-chat, Llama2-13b-chat (Touvron et al., 2023), and Llama3-8b-instruct (Grattafiori et al., 2024). To extract the internal states required for attribution, we re-process the model-generated responses in a teacher-forcing manner.

**Feature Extraction and Classifier.** For each response, we extract the 7-dimensional attribution vector for every token and aggregate them based on 18 universal POS tags (e.g., NOUN, VERB) defined by the SpaCy library (Honnibal et al., 2020). This results in a fixed-size feature vector ( $7 \times 18 = 126$  dimensions) for each sample. We employ XGBoost (Chen and Guestrin, 2016) as the binary classifier for hallucination detection due to its robustness on tabular data.

**Training and Evaluation Protocols.** To ensure fair comparison and rigorous evaluation, we tailor our training strategies to the data availability of each dataset. We implement strict data isolation protocols to prevent any form of data leakage, particularly for scenarios where official training splits are unavailable.

**Protocol I: Standard Split (RAGTruth Llama2-7b/13b).** For these datasets, we utilize the official train/test splits provided by prior work (Sun et al., 2025).

---

**Algorithm 1** SPAD Part I: Token-by-Token Generation and Probability Decomposition

---

**Require:** Transformer  $\mathcal{M}$ , Query Tokens  $\mathbf{x}_{\text{qry}}$ , Retrieved Context Tokens  $\mathbf{x}_{\text{rag}}$

**Ensure:** Sequence of 7-source attribution vectors  $\mathcal{V} = (\mathbf{v}_1, \dots, \mathbf{v}_T)$

```
1: Initialize context  $\mathbf{C} \leftarrow [\mathbf{x}_{\text{qry}}, \mathbf{x}_{\text{rag}}]$  and attribution storage  $\mathcal{V} \leftarrow \emptyset$ 
2: for step  $t = 1, 2, \dots$  until EOS do
3:   1. Forward Pass & State Caching
4:   Predict next token  $y_t$  using context  $\mathbf{C}$ .
5:   // Crucial: Save all intermediate residual states and attention maps for attribution
6:   Cache  $\mathbf{H}^{(0)}$ ,  $\mathbf{H}_{\text{mid}}^{(l)}$ ,  $\mathbf{H}^{(l)}$ , and Attention Maps  $\mathbf{A}^{(l)}$  for all layers  $l \in [1, L]$ .
7:   2. Coarse Decomposition (Residual Stream)
8:   Initialize  $\mathbf{v}_t \in \mathbb{R}^7$  with zeros.
9:    $\mathbf{v}_t[\text{Init}] \leftarrow \text{Probe}(\mathbf{H}^{(0)}, y_t)$  {Contribution from initial embedding}
10:   $\mathbf{v}_t[\text{LN}] \leftarrow P_{\text{final}}(y_t) - \text{Probe}(\mathbf{H}^{(L)}, y_t)$  {Contribution from final LayerNorm}
11:  3. Layer-wise Attribution
12:  for layer  $l = 1$  to  $L$  do
13:    // Calculate FFN contribution by probing states before and after FFN block
14:     $\mathbf{v}_t[\text{FFN}] += \text{Probe}(\mathbf{H}^{(l)}, y_t) - \text{Probe}(\mathbf{H}_{\text{mid}}^{(l)}, y_t)$ 
15:    // Calculate Total Attention contribution for this layer
16:     $\Delta P_{\text{att}} \leftarrow \text{Probe}(\mathbf{H}_{\text{mid}}^{(l)}, y_t) - \text{Probe}(\mathbf{H}^{(l-1)}, y_t)$ 
17:    4. Fine-Grained Decomposition (Head & Source)
18:    for head  $h = 1$  to  $H$  do
19:      // a. Head Attribution: How much did this head contribute to the target logit?
20:      Let  $\mathbf{o}_h$  be the output vector of head  $h$ .
21:      Compute logit update:  $\Delta z_h \leftarrow \mathbf{o}_h \cdot \text{UnbeddingVector}(y_t)$ 
22:      Compute ratio  $\omega_h \leftarrow \frac{\exp(\Delta z_h)}{\sum_j \exp(\Delta z_j)}$  {Logit-based apportionment}
23:       $\Delta P_h \leftarrow \Delta P_{\text{att}} \times \omega_h$ 
24:      // b. Source Mapping: Where did this head look?
25:      for source  $S \in \{\text{Qry}, \text{RAG}, \text{Past}, \text{Self}\}$  do
26:        Sum attention weights on indices of  $S$ :  $W_{h,S} \leftarrow \sum_{k \in \mathcal{I}_S} \mathbf{A}_h^{(l)}[t, k]$ 
27:        Normalize:  $\alpha_S \leftarrow W_{h,S} / \sum_{\text{all sources}} W_{h,\cdot}$ 
28:         $\mathbf{v}_t[S] += \Delta P_h \times \alpha_S$ 
29:      end for
30:    end for
31:  end for
32:  Append  $\mathbf{v}_t$  to  $\mathcal{V}$  and update context  $\mathbf{C} \leftarrow [\mathbf{C}, y_t]$ .
33: end for
34: return  $\mathcal{V}$ , Generated Tokens  $\mathbf{y}$ 
```

---

- **Optimization:** We perform hyperparameter optimization strictly on the training set using RandomizedSearchCV implemented in Scikit-learn (Pedregosa et al., 2011). We search for 50 iterations with an internal 5-fold cross-validation to maximize the F1-score.

- **Training:** The final model is trained on 85% of the training data using the best hyperparameters, with the remaining 15% serving as a validation set for early stopping (patience=50) to prevent overfitting.

- **Evaluation:** Performance is reported on the held-out official test set.

**Protocol II: Stratified 20-Fold CV (RAGTruth Llama3-8b).** As only test samples are publicly available for the Llama3-8b subset, we adopt a rigorous Stratified 20-Fold Cross-Validation scheme to maximize statistical power while maintaining evaluation integrity.

- **Strict Isolation:** In each of the 20 iterations, the dataset is partitioned into 95% training and 5% testing. Crucially, hyperparameter

---

**Algorithm 2** SPAD Part II: Syntax-Aware Feature Aggregation with Sub-word Tag Propagation

---

**Require:** Generated Tokens  $\mathbf{y} = (y_1, \dots, y_T)$ , Attribution Vectors  $\mathcal{V} = (\mathbf{v}_1, \dots, \mathbf{v}_T)$

**Ensure:** Syntax-Aware Feature Vector  $\mathbf{f} \in \mathbb{R}^{126}$

```
1: 1. String Reconstruction & Alignment Map
2: Decode tokens  $\mathbf{y}$  into a complete string text  $S$ .
3: Construct an alignment map  $M$  where  $M[i]$  contains the list of token indices corresponding to the
    $i$ -th word in  $S$ .
4: // Example: "modi" (idx 5), "fication" (idx 6)  $\rightarrow$  Word "modification" (idx  $w$ ); so  $M[w] = [5, 6]$ 
5: 2. POS Tagging & Propagation
6: Initialize tag list  $\mathcal{T}$  of length  $T$ .
7: Run POS tagger (e.g., SpaCy) on string  $S$  to obtain words  $W_1, \dots, W_K$  and tags  $\text{tag}_1, \dots, \text{tag}_K$ .
8: for each word index  $k = 1$  to  $K$  do
9:   Get corresponding token indices:  $\mathcal{I}_{\text{tokens}} \leftarrow M[k]$ 
10:  Get POS tag for the word:  $c \leftarrow \text{tag}_k$ 
11:  for each token index  $t \in \mathcal{I}_{\text{tokens}}$  do
12:     $\tau_t \leftarrow c$  {Propagate parent word's tag to all sub-word tokens}
13:  end for
14: end for
15: 3. Syntax-Aware Aggregation
16: Initialize feature vector  $\mathbf{f} \leftarrow \emptyset$ .
17: Define set of Universal POS tags  $\mathcal{P}_{\text{univ}}$ .
18: for each POS category  $c \in \mathcal{P}_{\text{univ}}$  do
19:   Identify tokens belonging to this category:  $\mathcal{I}_c = \{t \mid \tau_t = c\}$ 
20:   if  $\mathcal{I}_c \neq \emptyset$  then
21:     // Compute mean attribution profile for this syntactic category
22:      $\bar{\mathbf{v}}_c \leftarrow \frac{1}{|\mathcal{I}_c|} \sum_{t \in \mathcal{I}_c} \mathbf{v}_t$ 
23:   else
24:      $\bar{\mathbf{v}}_c \leftarrow \mathbf{0}_7$  {Fill with zeros if category is absent in response}
25:   end if
26:    $\mathbf{f} \leftarrow \text{Concatenate}(\mathbf{f}, \bar{\mathbf{v}}_c)$ 
27: end for
28: return  $\mathbf{f}$ 
```

---

optimization is performed anew for *each fold* using only that fold's training partition.

- **Aggregation:** The final metrics are calculated by micro-averaging the predictions across all 20 held-out test folds, ensuring every sample is evaluated exactly once as an unseen test instance.

**Protocol III: Nested Leave-One-Out CV (Dolly).**

To ensure a fair comparison with the benchmark established by (Sun et al., 2025), we strictly adhere to their experimental setting, which relies exclusively on a curated test set of 100 samples. Given the limited size of this specific evaluation split, we implement a **Nested Leave-One-Out Cross-Validation** to ensure statistical robustness.

- **Outer Loop (Evaluation):** We iterate 100

times. In each iteration, a single sample is strictly isolated as the test case.

- **Inner Loop (Optimization):** On the remaining 99 samples, we conduct an independent Bayesian hyperparameter search using Optuna (Akiba et al., 2019) for 50 trials. This inner loop uses its own 5-fold cross-validation to find the optimal configuration.
- **Class Imbalance:** To address the label imbalance in Dolly, we dynamically adjust the `scale_pos_weight` parameter in XGBoost based on the class distribution of the training fold.
- **Inference:** A model is trained on the 99 samples using the best parameters found in the inner loop and evaluated on the single held-out

sample. This process is repeated for all 100 samples to aggregate the final performance metrics.

## D Baselines Introduction

1. **EigenScore/INSIDE**(Chen et al., 2024) Focus on detecting hallucination by evaluating response’s semantic consistency, which is defined as the logarithm determinant of covariance matrix LLM’s internal states during generating the response.
2. **SEP**(Han et al., 2024) Proposed a linear model to detect hallucination based on semantic entropy in test time without requiring multiple responses.
3. **SAPLMA**(Azaria and Mitchell, 2023) Detecting hallucination based on the hidden layer activations of LLMs.
4. **ITI**(Li et al., 2023) Detecting hallucination based on the hidden layer activations of LLMs.
5. **Ragtruth Prompt**(Niu et al., 2024) Provides prompts for a LLM-as-judge to detect hallucination in RAG setting.
6. **LMvLM**(Cohen et al., 2023) It uses prompt to conduct a multiturn interaction between an examiner LLM and examinee LLM to reveal inconsistencies which implies hallucination.
7. **ChainPoll**(Friel and Sanyal, 2023) Provides prompts for a LLM-as-judge to detect hallucination in RAG setting.
8. **RAGAS**(Es et al., 2024) It uses a LLM to split the response into a set of statements and verify each statement is supported by the retrieved documents. If any statement is not supported, the response is considered hallucinated.
9. **Trulens**(TrueLens, 2024) Evaluating the overlap between the retrieved documents and the generated response to detect hallucination by a LLM.
10. **P(True)**(Kadavath et al., 2022) The paper detects hallucinations by having the model estimate the probability that its own generated answer is correct, based on the key assumption that it is often easier for a model to recognize a correct answer than to generate one.
11. **SelfCheckGPT**(Manakul et al., 2023) Self-CheckGPT detects hallucinations by checking for informational consistency across multiple stochastically sampled responses, based on the assumption that factual knowledge leads to consistent statements while hallucinations lead to divergent and contradictory ones.
12. **LN-Entropy**(Malinin and Gales, 2021) This paper detects hallucinations by quantifying knowledge uncertainty, which it measures primarily with a novel metric called Reverse Mutual Information that captures the disagreement across an ensemble’s predictions, with high RMI indicating a likely hallucination.
13. **Energy**(Liu et al., 2020) This paper detects hallucinations by using an energy score, derived directly from the model’s logits, as a more reliable uncertainty measure than softmax confidence to identify out-of-distribution inputs that cause the model to hallucinate.
14. **Focus**(Zhang et al., 2023) This paper detects hallucinations by calculating an uncertainty score focused on keywords, and then refines it by propagating penalties from unreliable context via attention and correcting token probabilities using entity types and inverse document frequency to mitigate both overconfidence and underconfidence.
15. **Perplexity**(Ren et al.) This paper detects hallucinations by separately measuring the Relative Mahalanobis Distance for both input and output embeddings, based on the assumption that in-domain examples will have embeddings closer to their respective foreground (in-domain) distributions than to a generic background distribution.
16. **REFCHECKER**(Hu et al., 2024) It uses a LLM to extract claim-triplets from a response and verify them by another LLM to detect hallucination.
17. **REDEEP**(Sun et al., 2025) It detects hallucination by analyzing the balance between the contributions from Copying Heads that process external context and Knowledge FFNs that inject internal knowledge, based on the finding that RAG hallucinations often arise from conflicts between these two sources. This method has two versions: token level and

chunk level. We compare with the latter since it has better performance generally.

## E Complexity Analysis of the Attribution Process

In this section, we rigorously analyze the computational overhead of our attribution framework. We focus strictly on the attribution extraction process for a generated response of length  $T$ . Let  $L$ ,  $d$ ,  $V$ , and  $H$  denote the number of layers, hidden dimension, vocabulary size, and attention heads (per layer), respectively. The standard inference complexity for a Transformer is  $\mathcal{O}(L \cdot T \cdot d^2 + L \cdot H \cdot T^2)$ . Our attribution process introduces post-hoc computations, decomposed into three specific stages:

**1. Exact Probability Decomposition.** To satisfy Theorem 1, we must compute the exact probability changes using the probe function  $\Phi(\mathbf{h}, y)$ . The bottleneck is the calculation of the global partition function (denominator) in Softmax.

- **Mechanism:** The probe function  $\Phi(\mathbf{h}, y) = \text{Softmax}(\mathbf{W}_u \mathbf{h})_y = \frac{\exp(\mathbf{w}_{u,y}^\top \mathbf{h})}{\sum_{v=1}^V \exp(\mathbf{w}_{u,v}^\top \mathbf{h})}$  requires projecting the hidden state  $\mathbf{h}$  to the full vocabulary logits  $\mathbf{z} = \mathbf{W}_u \mathbf{h}$ .
- **Single Probe Complexity:** For a single hidden state  $\mathbf{h} \in \mathbb{R}^d$ , the matrix-vector multiplication with the unembedding matrix  $\mathbf{W}_u \in \mathbb{R}^{V \times d}$  costs  $\mathcal{O}(V \cdot d)$ .
- **Total Calculation:** We must apply this probe at multiple points:
  1. **Global Components:** For  $P_{\text{initial}}$  and  $\Delta P_{\text{LN}}$ , the probe is called once per generation step. Cost:  $\mathcal{O}(T \cdot V \cdot d)$ .
  2. **Layer Components:** For  $\Delta P_{\text{att}}^{(l)}$  and  $\Delta P_{\text{ffn}}^{(l)}$ , the probe is invoked twice per layer (before and after the residual update). Summing over  $L$  layers, this costs  $\mathcal{O}(L \cdot T \cdot V \cdot d)$ .

- **Stage Complexity:** Combining these terms, the dominant complexity is  $\mathcal{O}(L \cdot T \cdot V \cdot d)$ .

**2. Head-wise Attribution.** Once  $\Delta P_{\text{att}}^{(l)}$  is obtained, we apportion it to individual heads based on their contribution to the target logit.

- **Mechanism:** This attribution requires projecting the target token embedding  $\mathbf{w}_{e,y}$  back into the hidden state space using the layer’s output projection matrix  $\mathbf{W}_O \in \mathbb{R}^{d \times d}$ .

- **Step Complexity:** The calculation proceeds in two sub-steps:

1. **Projection:** We compute the projected target vector  $\mathbf{g} = \mathbf{W}_O^\top \mathbf{w}_{e,y}$ . Since  $\mathbf{W}_O$  is a  $d \times d$  matrix, this matrix-vector multiplication costs  $\mathcal{O}(d^2)$ .
2. **Assignment:** We distribute the contribution to  $H$  heads by performing dot products between the head outputs  $\mathbf{o}_h$  and the corresponding segments of  $\mathbf{g}$ . For  $H$  heads, this sums to  $\mathcal{O}(d)$ .

- **Stage Complexity:** The projection step ( $\mathcal{O}(d^2)$ ) dominates the assignment step ( $\mathcal{O}(d)$ ). Integrating over  $L$  layers and  $T$  tokens, the total complexity is  $\mathcal{O}(L \cdot T \cdot d^2)$ .

**3. Mapping Attention to Input Sources.** Finally, we map head contributions to the four sources by aggregating attention weights  $\mathbf{A} \in \mathbb{R}^{H \times T \times T}$ . This involves two distinct sub-steps for each generated token at step  $t$  within a single layer:

- **Step 1: Summation.** For each head  $h$ , we sum the attention weights corresponding to specific source indices (e.g.,  $\mathcal{I}_{\text{RAG}}$ ):

$$w_{h,S} = \sum_{k \in \mathcal{I}_S} \mathbf{A}_h[t, k]$$

This requires iterating over the context length  $t$ . For  $H$  heads, the cost is  $\mathcal{O}(H \cdot t)$ .

- **Step 2: Normalization & Weighting.** We calculate the final source contribution by weighting the head contributions:

$$\Delta P_S = \sum_{h=1}^H \Delta P_h \cdot \frac{w_{h,S}}{\sum_{\text{all sources}} w_h}$$

This involves scalar operations proportional to the number of heads  $H$ . Cost:  $\mathcal{O}(H)$ .

- **Stage Complexity:** The summation step ( $\mathcal{O}(H \cdot t)$ ) dominates. We sum this cost across all  $L$  layers, and then accumulate over the generation steps  $t = 1$  to  $T$ . The calculation is  $\sum_{t=1}^T (L \cdot H \cdot t) \approx \mathcal{O}(L \cdot H \cdot T^2)$ .

**Overall Efficiency.** The total computational cost is the sum of these three stages:

$$\mathcal{C}_{\text{total}} = \underbrace{\mathcal{O}(L \cdot T \cdot V \cdot d)}_{\text{Prob. Decom.}} + \underbrace{\mathcal{O}(L \cdot T \cdot d^2)}_{\text{Head Attr.}} + \underbrace{\mathcal{O}(L \cdot H \cdot T^2)}_{\text{Source Map}}$$

**Runtime Efficiency.** It is worth noting that theoretical complexity does not directly equate to wall-clock latency. Standard text generation is *serial* (token-by-token), which limits GPU parallelization. In contrast, our framework process the full sequence of length  $T$  in a single parallel pass. This allows us to leverage efficient matrix operations on GPUs. Consequently, our single analysis pass is significantly faster in practice than baselines like SelfCheckGPT, which require running the slow serial generation process  $K$  times.